Influence of an electron-phonon subsystem on specific heat and two-photon absorption of the semimagnetic semiconductors $Pb_{1-x}Yb_xX$ (X=S, Se, Te) near the semiconductor-isolator phase transformation

K. Nouneh,[1,2] I. V. Kityk,[3] R. Viennois,[2,5] S. Benet,[1] S. Charar,[2] S. Paschen,[5] and K. Ozga[4]
[1]*Laboratoire de Physique Appliquée et Automatique, Université de Perpignan, 52 Avenue Paul Alduy, Perpignan, France*
[2]*Groupe d'Etude des Semiconducteurs, CNRS-UMR 5650, Université Montpellier II, Pl. Eugène Bataillon, 34095 Montpellier Cedex 5, France*
[3]*Institute of Physics, J. Dlugosz University of Czestochowa, Aleja Aermii Krajowej 13/15, Czestochowa, Poland*
[4]*Institute of Biology and Biophysics, Technical University Czestochowa, Aleja Armii Krajowej 36, Czestochowa, Poland*
[5]*Max-Planck-Institut für Chemische Physik Fester Stoffe, Nöthnitzer Strasse 40, 01185 Dresden, Germany*
(Received 23 March 2005; revised manuscript received 18 November 2005; published 26 January 2006)

Specific heat, transport, and two-photon absorption (TPA) effects were studied in single crystalline magnetic semiconductors $Pb_{1-x}Yb_xX$ (X=S, Se, Te at x=1–3%) near semiconductor-isolator phase transitions. It was shown that the TPA may be used as a sensitive tool for investigations of electron-phonon interactions near low temperature semiconductor-isolator phase transformation. Comparison with other methods of phase transition studies has shown more sharplike temperature dependence of the TPA. Particularly, comparison with piezo-optical and dilatometric methods shows on a better temperature resolution of the TPA with respect to the phase transitions. It was established as a correlation between the density of low-temperature phonon modes and values of the TPA. Particularly with increasing of the electron-phonon interactions defined by the temperature-dependent Debye term (parameter β) from the equation $C=\gamma T+\beta T^3+\Sigma_{i=1}^{n}\delta_i T^{2i+3}$, one can observe an increase of the TPA oscillator strengths. It was shown that only the low-temperature TPA behaviors might be determined by the features of the low-energy phonon modes related to the observed phase transformation. We also have discovered that low-temperature dependence of the specific heat C_p in $Pb_{1-x}R_xTe$ (R=Yb, Te) with x=2.6% and 1.65%, respectively, exhibits a nonmagnetic ordering caused by large value of electron-phonon contribution. Applying magnetic fields up to 2 T substantially modifies the temperature features of several phonon low-frequency modes, which may indicate a contribution of magnons.

DOI: 10.1103/PhysRevB.73.035329 PACS number(s): 42.65.Ky, 73.40.Qv

I. INTRODUCTION

Semimagnetic semiconductors (SMSs) [also known as diluted magnetic semiconductors (DMSs)] are single crystalline semiconductor solid solutions where a part of the cations is replaced by transition metals or rare earth ions. We investigated DMS single crystalline samples of $Pb_{1-x}R_xX$ (X=S, Se, Te and R=Yb, Pr) in which a part of the Pb^{2+} ions were replaced by Yb^{3+} (Pr^{3+}). All these materials have the rock-salt crystalline structure (NaCl-structural type). The electronic configuration of Yb^{3+} is $4f^{13}$ (L=3, S=1/2). The average Yb^{3+} (Pr^{3+}) valence states are equal to about 3+. In this case, the Yb^{3+} (Pr^{3+}) ions are disproportionate to the valence of Pb^{2+} and the Yb^{3+} (Pr^{3+}) impurity levels form resonant states close to the top of the valence band, pinning the Fermi level and strongly affecting the transport and thermal properties.[1–4] In the case of rare-earth (RE) impurities, the energy of electron states depend primarily on the Coulomb interaction between the localized f RE electrons of the solute.[5] However, the weaker coupling between the solute and host states may play a crucial role for the valence state of the RE impurities, assuming that energy of the corresponding excited states are low.[6] A crucial point here is also magnetic state of the rare-earth ions. For example, if one electron leaves the f shell of RE^{3+}, the resulting localized moment is coupled through exchange interaction with spins of the remaining delocalized electrons. It is well known that spin fluctuations give rise to a Kondo anomaly-strong coupling between the magnetic moment of the solute and quasifree electrons. However, charge fluctuations, if significant, suppress Kondo anomalies and result in heterovalent states.

Third-order nonlinear optic methods, and particularly, two-photon absorption (TPA) determined by the imaginary part of third-order susceptibility $\chi^{(3)}$ were recently widely used for investigation of the effective electron-phonon interaction during different phase transitions.[7,8] It is caused by the fact that multiphoton quantum transitions effectively interact with the boson subsystem. Because, near the critical points, density of bosons usually is drastically changed, one can expect an occurrence of singularities in corresponding temperature dependences of nonlinear optical susceptibilities.

It is necessary to emphasize that the investigated semimagnetic crystals seem to be very promising like thermoelectric materials. The key parameter here is a figure of merit for thermoelectric performance Z, which is proportional to effective mass of the carriers m^*, their mobility μ, and thermal conductivity due to phonon κ according to the relation

$$Z \propto m^{*3/2}\frac{\mu}{\kappa}. \quad (1)$$

Thus, the determination of these parameters may allow us to find a maximum of Z following an optimum cationic substitution. The thermal conductivity due to the phonon depends

mainly on the mechanism of electron-phonon diffusion. So high a value of Z will be possible in the material with higher effective masses and lower thermal conductivity, like semimagnetic semiconductors or heavy fermion compounds.

Generally the TPA determined by the imaginary part of third-order optical susceptibility is described by a fourth-rank polar tensor. The macroscopic susceptibility is related with microscopic hyperpolarizability by a relation[9]

$$\chi_{ijkl} = L_i L_j L_k L_l \gamma_{ijkl}, \tag{2}$$

where $L_{i,j,k,l}$ are ith, jth, kth, and lth local field Lorentz components; γ_{ijkl} is the microscopic third-order hyperpolarizability.

Generally within the framework of the simple three-band model, the hyperpolarizability γ_{ijkl} is related to the principal microscopic parameters by an approximate equation

$$\gamma_{ijkl} = \sum_{\vec{k}} \frac{\vec{\mu}_i \vec{\mu}_j \Delta\vec{\mu}_k \Delta\vec{\mu}_l}{E_g^{\,3}}, \tag{3}$$

where $\vec{\mu}_i$ is the ith component of transition dipole moment for optical transition between the levels forming efficient energy gap E_g; $\Delta\vec{\mu}_l$ is the difference between the excited and ground dipole moments for the levels forming the efficient interband energy interval E_g. The contribution from the different points of the band structure is summarized and renormalized over the number of summated points k in the Brillouin zone (BZ). The dipole moments have two parts—one strong electronic which is only slightly dependent on temperature and one phonon part which is very sensitive to occurrence of phonon or magnon modes, particularly near the tricritical points or phase transitions. It is well known that near the critical temperature T_c several phonon modes (so-called "soft" phonon modes) have singularlike temperature dependence

$$n_{ph} \approx |T - T_c|^{-\gamma}, \tag{4}$$

where power parameter γ is strongly dependent on the origin of the particular phase transformation.

It is a main reason why boson modes are extremely sensitive to different phase transformations. Particularly, in the case of the spin-correlated subsystems, additional contributions also give magnons. It reflects the fact that near the critical temperature of the phase transition, the number of singularlike bosons (both phonons and magnons) drastically increases leading to the next increase of the nonlinear optical susceptibility described by Eq. (2). Due to the noninvasive features of the nonliner optical methods, they have substantial advantages compared to traditional thermodynamical and structural methods [like differential scanning calorimetry (DSC), x-ray, electron paramagnetic resonance (EPR), and NMR].

In the present paper, the TPA and thermal properties are investigated for $Pb_{1-x}Yb_xX$ (X=S, Se, Te and x=1–3%) compounds as well as for $Pb_{1-x}Pr_xTe$ (x=1.65%) and PbTe. The key goal of the work is to explore the TPA as a sensitive tool for studying the weak electron-phonon contribution to DMSs near the corresponding phase transition and to compare them with transport, thermodynamics, and several methods sensitive to the phase transitions. At the same time, we look for multifunctional materials possessing simultaneously excellent thermoelectric and nonlinear optical properties in the IR-spectral range.

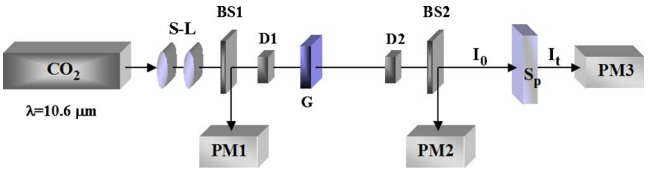

FIG. 1. (Color online) Principal experimental setup for the TPA measurements. **S-L**—system of collimating lenses, **PM**—photomultipliers, **G**—Glan Thompson polarizer, **BS**—beam splitters, $\mathbf{S_P}$—specimen kept in the thermoregulated helium cryostat, and **D**—density optical filter, **CO**2—fundamental CO_2 laser.

II. EXPERIMENTAL DETAILS

A. Synthesis of samples

Single crystals of $Pb_{1-x}Yb_xTe$, $Pb_{1-x}Yb_xSe$, and $Pb_{1-x}Yb_xS$ were grown using traditional Bridgman method. The sample dimensions were equal to about ($3\times2\times1.5$ mm^3), the longest axis was directed along the [001] direction. The Yb contents were equal to 0.18, 0.026 for $Pb_{1-x}Yb_xTe$ and 0.01 and 0.03 for $Pb_{1-x}Yb_xS$, $Pb_{1-x}Yb_xSe$, respectively, following the data of the microprobe analysis.

B. Transport and thermal properties

For the thermopower measurements of the Seebeck coefficient $S(T)$, we use the hot point method. The basic principle of the method is to create a variation in temperature ΔT in the sample using a hot point and to measure the voltage ΔV that results from the temperature variation. The Seebeck coefficient was determined by an expression $S=\Delta V/\Delta T$. The heat capacity measurements $C_P(T)$ between 0.4 and 300 K were done by a relaxation method using a microcalorimeter and a PPMS apparatus from Quantum Design.[9]

C. TPA measurements

We have performed the TPA measurements using a fundamental laser beam illumination of the pulsed (pulse duration 0.3 μs) CO_2 IR laser (see Fig. 1), which is transparent for the investigated samples at $\lambda=10.6$ μm. Average light power densities were equal to 10 MW/cm^2. The sample's temperature was monitored by a microthermobolometer chip with accuracy up to 0.2 K. This was done simultaneously from both sides of the samples. The highest observed local heating due to sample absorption did not exceed 0.8 K. Previously, it obtained almost the same value for different investigated metals and superconductors.[10,11]

The setup also allows a moving over the specimen's surface by the fundamental light beams. The beam profile sequence had a Gaussian-like shape with a half-width dispersion equal to about 78%. The laser power stability was kept stabilized within 0.1%. The values of the TPA coefficients

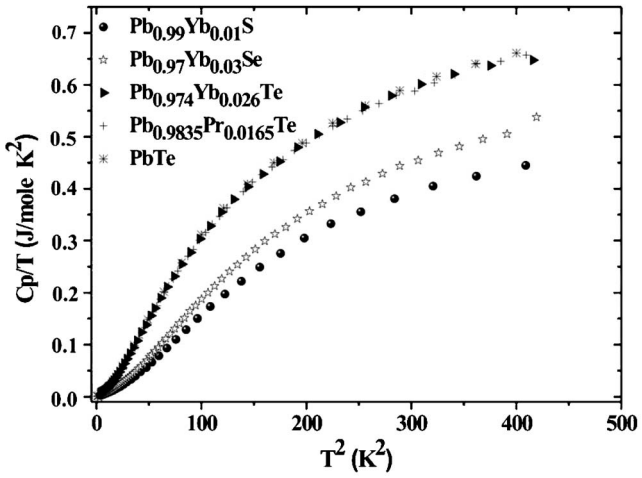

FIG. 2. Temperature dependence of specific heat (C_p/T vs T^2) for $Pb_{1-x}Yb_xX$ (X=S, Se, x=1–3%) and $Pb_{0.9835}Pr_{0.0165}Te$ (PbTe).

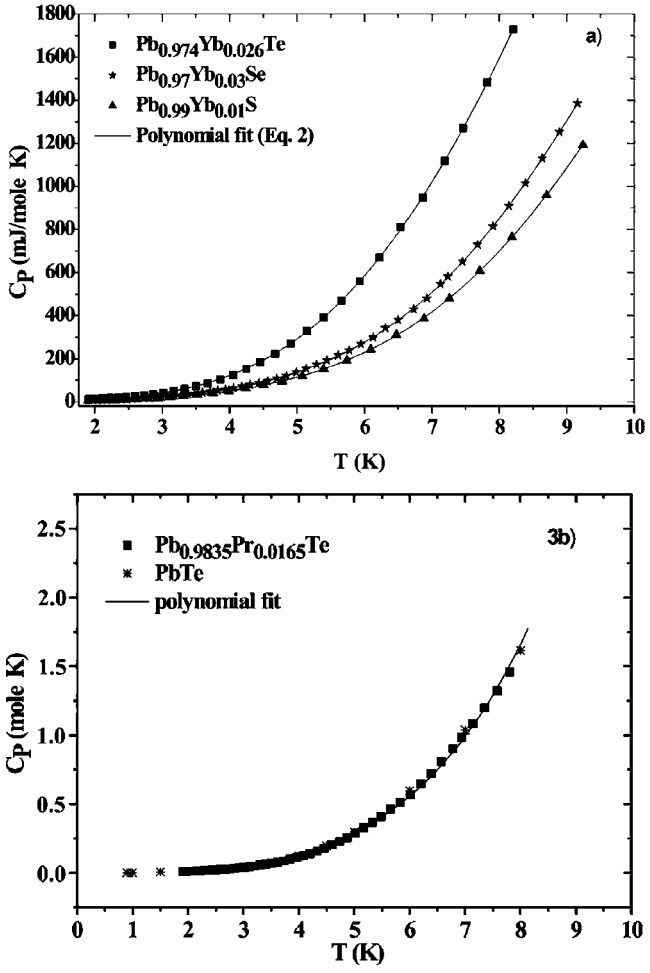

FIG. 3. (a) Heat capacity of $Pb_{1-x}Yb_xX$ (X=S, Se, x=1–3%) plotted vs T for $1.9 \leqslant T \leqslant 10$ K. The solid lines correspond to the polynomial fit using Eq. (6) (with n=3) at low temperatures taking in account the phonon contribution. (b) Heat capacity of $Pb_{0.9835}Pr_{0.0165}Te$ and PbTe plotted vs T for $1.9 \leqslant T \leqslant 10$ K. The solid lines correspond to the polynomial fit using Eq. (6) (with n =3) at low temperatures taking into account the phonon contribution.

were determined from pump dependences of the transparency T using an expression

$$T = 1 - BdI_p, \tag{5}$$

where B is the evaluated TPA coefficient; d is the sample thickness; and I_p is the power density of the pumping beam. The maximally achieved TPA values were achieved for parallel polarizations of the incident and output beams corresponding to diagonal tensor components of B.

III. RESULTS AND DISCUSSIONS

A. Thermal properties (Heat-capacity and the Seebeck coefficient)

Usually, low-temperature heat capacity can be described by an odd power series expansion with respect to temperature T

$$C = \gamma T + \beta T^3 + \sum_{i=1}^{n} \delta_i T^{2i+3}, \tag{6}$$

where C is a molar heat capacity in units of mJ/mol K; γ is the electronic coefficient of the heat capacity in mJ/mol K^2; β is the low-order lattice contribution (Debye term) in mJ/mol K^4; and the δ_i are the coefficients of the higher-order lattice terms arising from the dispersion of the low-frequency phonon modes. The Debye temperature is described by an expression

$$\Theta_D = (1944\upsilon/\beta)^{1/3}, \tag{7}$$

where υ is the number of atoms per molecule. For most of the materials at sufficiently low-temperature, Eq. (6) is reduced to

$$C = \gamma T + \beta T^3, \tag{8}$$

so that a plot C_P/T vs T^2 would yield a straight line with slope β and intercept γ

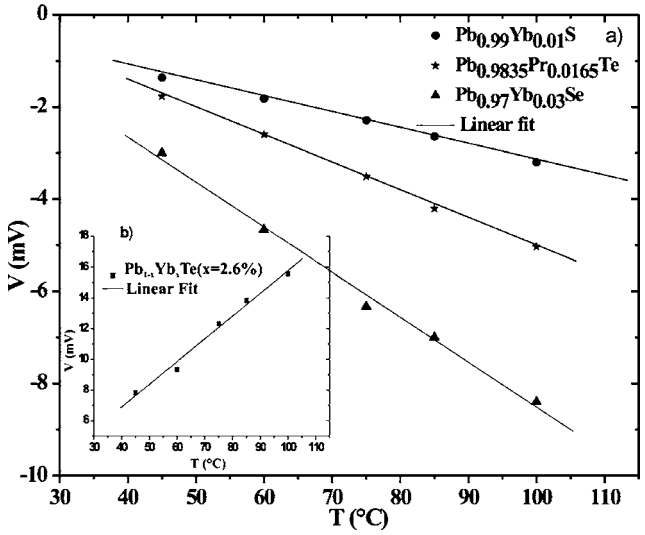

FIG. 4. Typical temperature dependence of the Seebeck coefficients.

TABLE I. Coefficients of best polynomial fit using Eq. (6) for the molar heat capacity of $Pb_{1-x}Yb_xX$ (X=S, Se, Te, x=1–3%), $Pb_{1-x}Pr_xTe$ (x=1.65%) and PbTe within temperature range 1.9–10 K.

Samples	γ [mJ/mol K^2]	β [mJ/mol K^4]	δ [mJ/mol K^6]	$\Theta_D(0)$ [K]
$Pb_{0.974}Yb_{0.026}Te$	0.15	0.8014	0.08386	169.28
	±0	±0.0744	$\pm 5.77\times10^{-3}$	±5.32
$Pb_{0.97}Yb_{0.03}Se$	0.45	0.6308	0.01785	183.34
	±0	±0.0197	$\pm 1.24\times10^{-3}$	±1.91
$Pb_{0.99}Yb_{0.01}S$	0.56	0.4939	0.01706	198.92
	±0	±0.0175	$\pm 1.08\times10^{-3}$	±2.35
$Pb_{0.9835}Pr_{0.0165}Te$	0.26	1.0358	0.05057	155.41
	±0	±0.0293	$\pm 1.06\times10^{-3}$	±1.46
PbTe	0.65	0.6807	0.09064	178.75
	±0	±0.0178	$\pm 1.17\times10^{-3}$	±1.56

$$C_P/T = \gamma + \beta T^2. \quad (9)$$

For all the materials, such a temperature feature could be found below 10 K. Attempts to fit the $C_P(T)$ data (see Fig. 2) for all the samples with an Eq. (9) were unsuccessful, because the fit did not reproduce satisfactorily the experimental data and give negative γ values. The best polynomial fit for the heat capacity of the samples was achieved with a precision up to 0.2%. Data for $Pb_{1-x}Yb_xX$ (X=S, Se, Te, x=1–3%), $Pb_{1-x}Pr_xTe$ (x=1.65%) and PbTe could be fit using Eq. (6) with n=3, within a temperature range from 1.9 to 10 K. The resulting variations are presented in the Fig. 3(a) and Fig. 3(b). The values of γ, β, δ_1, and $\Theta_D(0)$ for all the investigated samples are given in Table I, where $\Theta_D(0)$ was calculated from β and congruent values of v=2, using Eq. (7). The coefficients δ_2 and δ_3 are very small and not significant (equal to 10^{-6} mJ/mol K^7 and 10^{-8} mJ/mol K^9, respectively).

In Fig. 4, the temperature dependences of $\Delta V = f(\Delta T)$ for different samples are presented and corresponding data are shown in Table II. These results show that the Seebeck coefficient for $Pb_{1-x}Yb_xTe$ (S=148 μV/K) is larger than that for $Pb_{1-x}Yb_xX$ (X=Se, S) ($|S|$=97 μV/K, 37 μV/K), respectively. The negative sign indicates an n-type conductivity of material. However, for $Pb_{1-x}Yb_xTe$, the measurements show that the Seebeck coefficient is equal to 118 μV/K, which is almost two times larger than for $Pb_{1-x}Pr_xTe$ ($|S|$ =60 μV/K). The next paragraph will give the results of the corresponding temperature dependences of the TPA and additional measurements on the phonon mode temperature behaviors will be presented.

It is necessary to emphasize that the best polynomial fit of the experimental data was achieved for Eq. (6) with n=3, within the temperature range 1.9–10 K for PbTe. The θ_D =178.75±1.56 K is approximately equal to the values given by Houston *et al.*[12] (176.6±0.56 K) which confirms our results. Otherwise, one can see for the $Pb_{1-x}Yb_xX$ (X =S, Se, Te) that the Debye term β (Debye temperature θ_D) increases with increasing anion mass (^{16}S, ^{34}Se, ^{52}Te). It is necessary also to add that Debye terms for Pr compounds [β(Pr)=1.0358±0.0293 mJ/mol K^4] are larger than for Yb compounds [β(Yb)=0.8014±0.0744 mJ/mol K^4]. These results confirm the observed phenomena in the TPA measurements (see Figs. 5 and 6).

In Fig. 2, one can see clearly that Pr^{3+} are nonmagnetic in these compounds, but Yb compounds have a very low magnetic contribution into PbTe. Also, the Summerfield coefficients γ in the both samples are very low [γ(Yb) =0.15 mJ/mol K^2, γ(Pr)=0.26 mJ/mol K^2 in $Pb_{1-x}Yb_xTe$ and $Pb_{1-x}Pr_xTe$, respectively].

It is known that a substantial magnetic contribution to the C_p was observed in $Pb_{1-x}Mn_xTe$ below 1 K.[13] However, contrary to this case, in $Pb_{1-x}R_xTe$, (R=rare earth), the magnetic contribution is very low compared to the contribution of the phonon subsystem. However, from the electron paramagnetic resonance, a measurement carried out for PbX (X=S, Se, or Te) doped by Yb it was shown that the Yb ions possess substantial magnetic contributions in these compounds.[14] The signal discovered in the $Pb_{1-x}Mn_xTe$ (x=0.024 and 0.056) was attributed to the splitting of Mn levels about 1 K, due to *sp-d* exchange interaction.[15] In this model, the authors show that $T_{\max}^{C_r} \approx J|J_{NN}|$, in the case of Yb^{3+} (J=7/2), and $J_{NN} \approx -0.5$ (±0.2) K^2. They expect to have a maximum below 2 K, but this maximum was not observed. Probably the authors were not familiar with the results of Escorne *et al.*,[16] indicating the existence of a transition toward a spin-glass state in the same range of temperature (below 0.25 and

TABLE II. Seebeck coefficients of $Pb_{1-x}Yb_xX$ (X=S, Se, Te, x=1–3%), $Pb_{1-x}Pr_xTe$ (x=1.65%) at room temperature.

	$Pb_{0.974}Yb_{0.026}Te$	$Pb_{0.9835}Pr_{0.0165}Te$	$Pb_{0.97}Yb_{0.03}Se$ (n type)	$Pb_{0.99}Yb_{0.01}S$ (n type)
S(μV/K)	148	−60	−97	−37

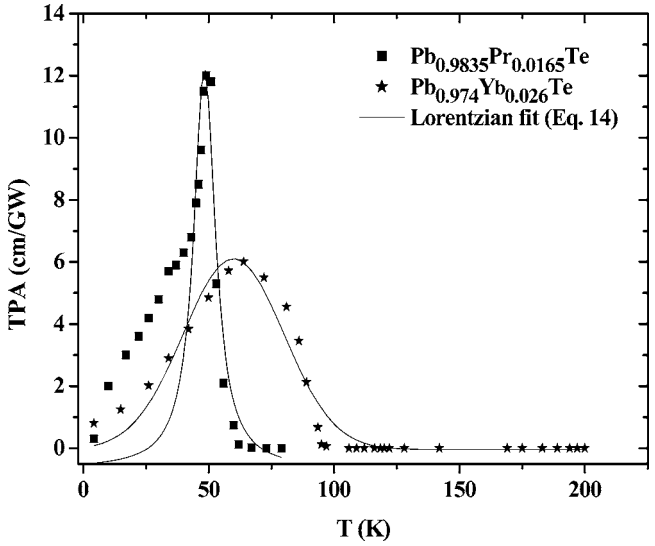

FIG. 5. Temperature dependence of TPA in $Pb_{0.974}Yb_{0.026}Te$ and $Pb_{0.9835}Pr_{0.0165}Te$. The solid lines correspond to the Lorentzian fit using Eq. (12).

1 K). The absence of an important magnetic signal in our samples and the existence of a large signal in nonlinear optics measurements (Figs. 5 and 6) confirm the approach of Escorne *et al.*[16]

B. Two-photon absorption

Generally, linear absorption of the light by a condensed matter is described by the equation

$$I_t = I_0 \cdot e^{-\alpha \cdot d}, \tag{10}$$

where α is the absorption coefficient; d is the thickness of the absorbing layer; I_0 and I_t are the incident and output light beam intensities, respectively.

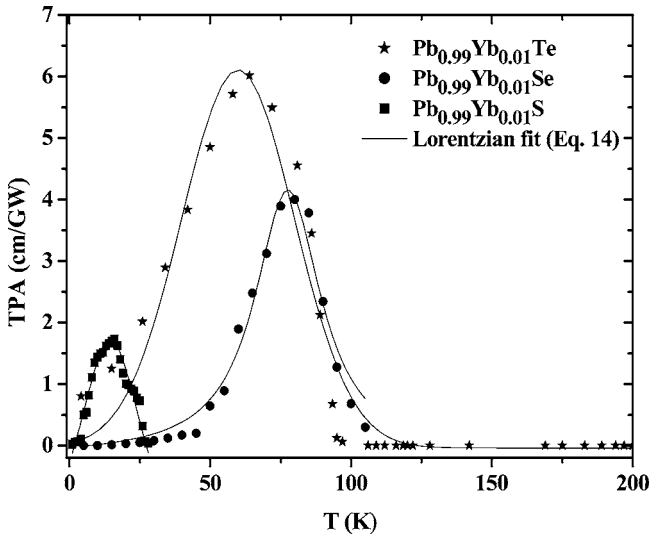

FIG. 6. Temperature dependence of TPA in $Pb_{1-x}Yb_xX$ (X = S, Se, x=1–3%). The solid lines correspond to the Lorentzian fit using Eq. (12).

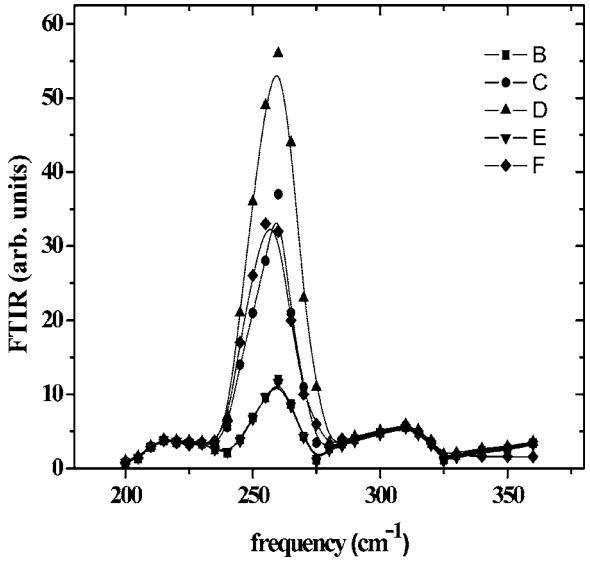

FIG. 7. Fragment of FTIR spectra vs temperature for PbPrTe single crystals at T=4.2 K—curve **B**, 35 K—**F**, 50 K—**D**, 80 K—**E**, in magnetic field of about 2 T at 50—**C**.

For the larger intensities of the electromagnetic wave, absorption can have a nonlinear character that is intensity dependent. In this case, the transparency of the light is a function of linear (α) and nonlinear (β) absorption parts. The latter is linearly related with the TPA coefficient,

$$T = \frac{I(d)}{I(0)} = \frac{\alpha \exp(-\alpha \cdot d)}{\alpha + \beta \cdot I(0) \cdot [1 - \exp(-\alpha \cdot d)]}. \tag{11}$$

The TPA is sensitive to the phonon contribution, which near the critical phase transition point has the singularlike temperature dependence [see Eq. (4)]. For convenience, such singularlike dependence may be presented in a Lorentzian-

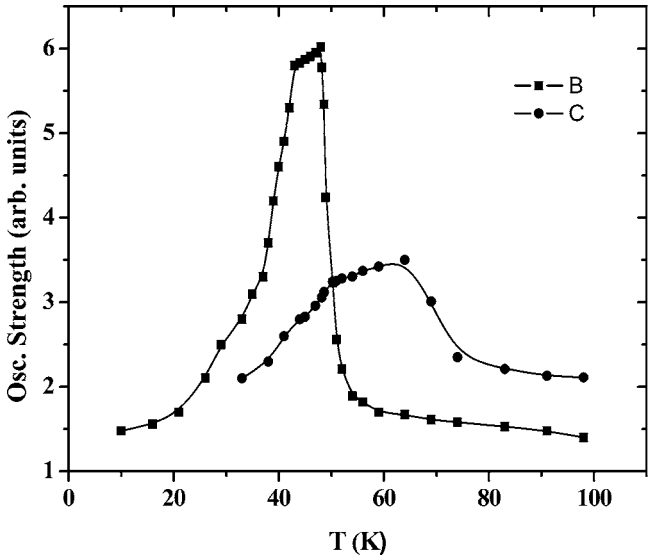

FIG. 8. Dependence of the oscillator strength for two sensitive phonon modes vs temperature: **B**—mode 262 cm^{-1} for the PbPrTe, **C**—mode 251 cm^{-1} for the PbYbTe.

TABLE III. Coefficients of Lorentzian fit using Eq. (14) for the low temperature TPA measurements of $Pb_{1-x}Yb_xX$ (X=S, Se, Te, x=1–3%) and $Pb_{1-x}Pr_xTe$ (x=1.65%).

	$Pb_{0.9835}Pr_{x0.0165}Te$	$Pb_{0.974}Yb_{0.026}Te$	$Pb_{0.97}Yb_{0.03}Se$	$Pb_{0.99}Yb_{0.01}S$
T_c (K)	48.324	59.878	77.564	14.538
	±0.753	±1.046	±0.592	±0.193
Γ	10.500	40.05494	28.7474	31.036
	±2.900	±2.29872	±2.5229	±6.317
A	211.757	308.471	195.242	207.435
	±60.773	±19.500	±17.642	±92.559
y_o	−0.653	−0.039	−0.169	−2.542
	±0.1.00	±0.013	±0.012	±1.071

like temperature-dependent form[17] (see Figs. 5 and 6). The TPA versus the temperature may be presented like the dependence of effective oscillators (determined by the corresponding dipole moments) versus temperature. In this case, the intensity of the TPA will be determined by the oscillator strengths directly related with the temperature feature of the dipole moments due to phonon contribution (temperature-sensitive) part. The latter parts (phonon and magnon dependent) determine Lorenzian-like temperature dependence of the TPA near the critical point T_c. One can expect that the phonon contribution to the C_p through the Debye factor should correlate well with the temperature concerning the TPA oscillator strengths.

To clarify the role played by the phonon subsystem, additional investigations of the Fourier transform infrared (FTIR) spectra versus temperature were done. Particularly from Fig. 7, one can clearly see that the low-energy IR spectral fragment (at about 260 cm^{-1} for the PbPrTe) demonstrates a drastic enhancement of phonon oscillator strength (determined by the spectral curve planes of the corresponding phonon modes). These modes manifest high sensitivity to the occurrence of phase transition near the low- temperature critical point. The 260 cm^{-1} phonon mode corresponding to stretching phonons originating from PbPrTe drastically enhances its oscillator strength in the temperature range 4.2–45 K and again decreases below 75 K. So it is in agreement with the TPA temperature behavior shown in Fig. 5.

Moreover to verify the possible magnon participation in the processes observed, additional investigations on the influence of the magnetic field up to 2 T were performed. From the Fig. 7, one can see that the magnetic field up to 2 T does not only change the oscillator strengths; however, this also leads to a several-spectral shift of the corresponding FTIR dependences. The similar behavior was observed also for the phonon mode at 252 cm^{-1} in the case of the PbYbTe single crystals. From Fig. 7, it is clear that other modes are almost nonsensitive to the temperature of phase transition or applied magnetic field.

For convenience, we have presented dependences of the sensitive phonon oscillator strengths versus temperature (see Fig. 8). One can see that the temperature behaviors of the corresponding phonon oscillator strengths are in a sufficiently good agreement with the corresponding dependences of the TPA values. So comparing the data on the thermodynamical, transport, and nonlinear optical properties versus temperature with the behavior of the particular phonon modes, one can determine the principal role played by the low-energy phonon modes in the observed dependences. One can say that the TPA effects seem to be more sensitive compared to the transport or thermodynamic ones.

It was also shown that low-temperature TPA behavior could be simulated within a framework of the Lorentzian function form,

$$f(T) = y_0 + \frac{A}{2\pi}\frac{\Gamma}{(T-T_c)^2 + \left(\frac{\Gamma}{2}\right)^2}, \tag{12}$$

where Γ determines the Lorentzian line shape widening; T_c is the critical temperature of the phase transition; y_0 and A are numerical constants fitted to the experimental data.

Using the semiempirical function (12), we have simulated the temperature dependences of the phase transformations for all the investigated samples (see Table III).

From Figs. 5–8, one can see that we observe more electron-phonon (magnon) contributions for Pr^{3+} ions compared to the Yb^{3+} ones. And this correlates well with the

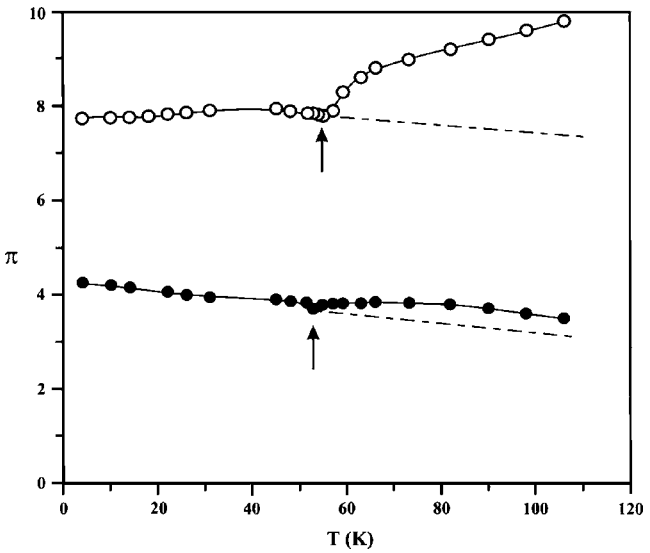

FIG. 9. Temperature dependences of longitudinal (open circles) and transverse (closed circles) thermal expansion coefficients π for the PbYbTe in arbitrary units.

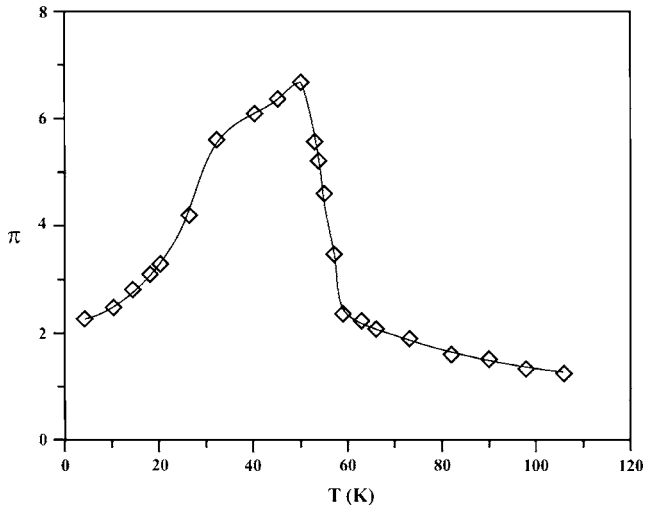

FIG. 10. Temperature dependences of longitudinal piezo-optical coefficient for the PbYbTe in the 10^{14} m^2/N.

Debye term (β) (electron-phonon contributions from C_p).[18–20]

Together with the temperature data on the Debye parameter, one can conclude that the temperature shift of the TPA is closely connected with the contribution of electron-phonon interaction. With increasing of the anionic mass, we also observe a temperature shift of the TPA oscillator strength toward the lower temperature.

In order to compare temperature sensitivity of the TPA to the observed phase transitions, we have performed temperature-dependent investigations for these compounds near the phase transitions. We have chosen dilatometric and piezo-optical methods which traditionally are used as sensitive tools of different phase transitions,[21,22] particularly they are sensitive to the local structural ordering. Figures 9 and 10 present the corresponding temperature dependences. The thermal expansion determined by dilatometric method[21] (see Fig. 9) demonstrates only slight breaks both for the longitudinal as well as transverse mechanical stress component. The piezo-optic coefficient at $\lambda = 10.6$ μm obtained by the Senarmont method[22] shows sharp temperature dependence. However, its width is substantially higher compared to the TPA. So precise determination of the temperature position of the PT's point seems to be more favorable using the TPA. It may be a consequence of higher sensitivity of multiphoton transitions to the interactions with boson subsystems compared to the mentioned methods.

IV. CONCLUSIONS

Complex investigations of transport properties, heat capacity, and nonlinear optical susceptibility in magnetic single-crystalline semiconductors $Pb_{1-x}Yb_xX$ (X=S, Se, Te at x=1–3%) versus temperature have shown that third-order nonlinear optical methods may be served as a sensitive tool for investigations of electron-phonon interactions near the low-temperature semiconductor-isolator phase transformation in semimagnetic semiconductors. It demonstrated a correlation between the temperature dependence of the thermodynamical parameters, TPA, and low-energy phonon modes using the FTIR method. We observed more electron-phonon contributions for Pr^{3+}-containing compounds compared to the Yb^{3+} ones. With increasing electron-phonon interactions indicated by temperature dependences of the β parameter, one can observe an increase of oscillator strengths for the TPA. Together with temperature data on the Debye parameter obtained from thermodynamical approaches, one can conclude that the temperature shift of the TPA is closely connected with the contribution of electron-phonon interaction with several admixtures of the magnons (due to demonstrated sensitivity to the applied magnetic field) and particularly to the electron-phonon interaction. With the increasing of anionic mass, we observe a temperature shift of the TPA oscillator strength toward the lower temperature.

To show substantial influence of the phonon and magnon subsystems on the output nonlinear optical susceptibilities, we have done temperature measurement of the FTIR We have established that there exists a soft mode at 262 cm^{-1} for the PbPrTe and 251 cm^{-1} for PbYbTe materials. Their temperature dependences are well correlated with the dependences of the TPA. At the same time, they show substantial sensitivity to the external magnetic field, which might indicate several contributions of the spin-correlated magnon subsystems. Precise determination of the temperature position of the PT's point seems to be more favorable using the TPA compared to such sensitive methods like piezo-optical or dilatometric effects. It may be a consequence of higher sensitivity of multiphoton transitions to the interactions with boson subsystems.

ACKNOWLEDGMENTS

We acknowledge helpful discussions with Professor F. Terki (Group Etudes Semiconductor GES, University Montpellier II, France) and Z. Golacki (Institute of Physics, Warsaw, Poland) for the sample preparations for very useful discussions and suggestions concerning the transport part of the paper. This research was supported in part by a contract from OTAN Polonium with the Army University of Warsaw (Poland) and University of Perpignan (France).

[1] B. Grover, Phys. Rev. **140**, A1944 (1965).
[2] C. Rettori, D. Davidov, and A. Grayevskey, Phys. Rev. B **11**, 4450 (1975).
[3] I. V. Kityk, W. Gruhn, and B. Sahraoui, Opt. Lasers Eng. **41**, 51 (2004).
[4] Y. Lubianiker and I. Balberg, Phys. Status Solidi B **205**, 119 (1998).
[5] A. L. Efros and B. I. Shklovskii, J. Phys. C **8**, L49 (1975).

[6] V. K. Dugaev, Inorg. Mater. **36**, 524 (2000).
[7] B. Sahraoui, I. Kityk, X. N. Phu, P. Hudhomme, and A. Gorgues, Phys. Rev. B **59**, 9229 (1999).
[8] I. V. Kityk, P. Bragiel, M. Piasecki, I. Fuks, B. Sahraoui, P. Hudhomme, and A. Gorgues, Phase Transitions **74**, 347 (2001).
[9] I. V. Kityk, J. Ebothe, A. H. Addou, A. Bougrine, and B. Sahraoui, Phys. Status Solidi B **234**, 353 (2002).
[10] I. Kityk, J. Phys.: Condens. Matter **6**, 4119 (1994).
[11] I. Kityk and E. Jakubczyk, Appl. Opt. **38**, 3152 (1999).
[12] B. Houston, R. E. Stranka, and H. S. Belson, J. Appl. Phys. **39**, 3913 (1968).
[13] A. Lusakowski, A. Jedrzejczak, M. Gorska, V. Osinniy, M. Arciszewska, W. Dobrowolski, V. Domukhovski, B. Witkowska, T. Story, and R. R. Galazka, Phys. Rev. B **65**, 165206 (2002).
[14] S. Isber, S. Charar, X. Gratens, C. Fau, M. Averous, S. K. Misra, and Z. Golacki, Phys. Rev. B **54**, 7634 (1996).
[15] M. Gorska and J. R. Anderson, Phys. Rev. B **38**, 9120 (1988); M. Gorska, J. R. Anderson, G. Kido, S. M. Green, and Z. Golacki, Phys. Rev. B **45**, 11702 (1992).
[16] M. Escorne, A. Mauger, J. L. Tholence, and R. Triboulet, Phys. Rev. B **29**, 6306 (1984).
[17] B. P. Antonyuk, Opt. Commun. **181**, 191 (2000).
[18] N. Primozich, T. V. Shahbazyan, I. E. Perakis, and D. S. Chemla, Phys. Rev. B **61**, 2041 (2000).
[19] H. Krogger, Springer Ser. Opt. Sci. **312**, 137 (2003).
[20] D. Dong Ling, *Phase Transformation in Optics* (Wiley, New York, 2003), p. 185.
[21] Y. V. Burak and I. E. Moroz, Phys. Chem. Glasses **44**, 241 (2003).
[22] V. B. Kapustinik, Phys. Status Solidi B **168**, 109 (1999).